LiDAR Remote Sensing Data Collection
Department of Geology and Mineral Industries
New Madrid Study Area
March 30th, 2012

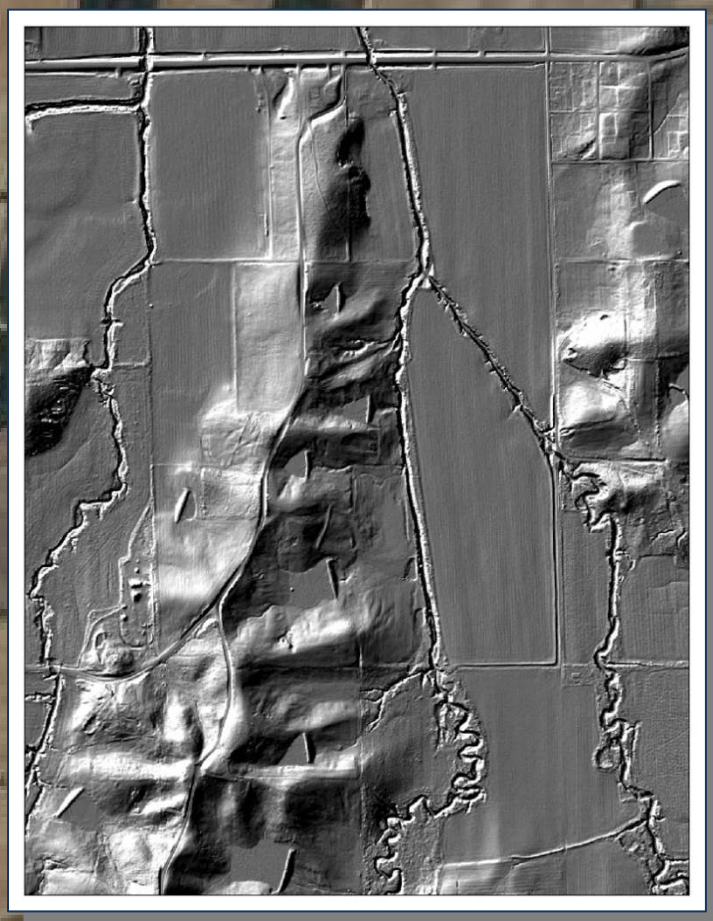

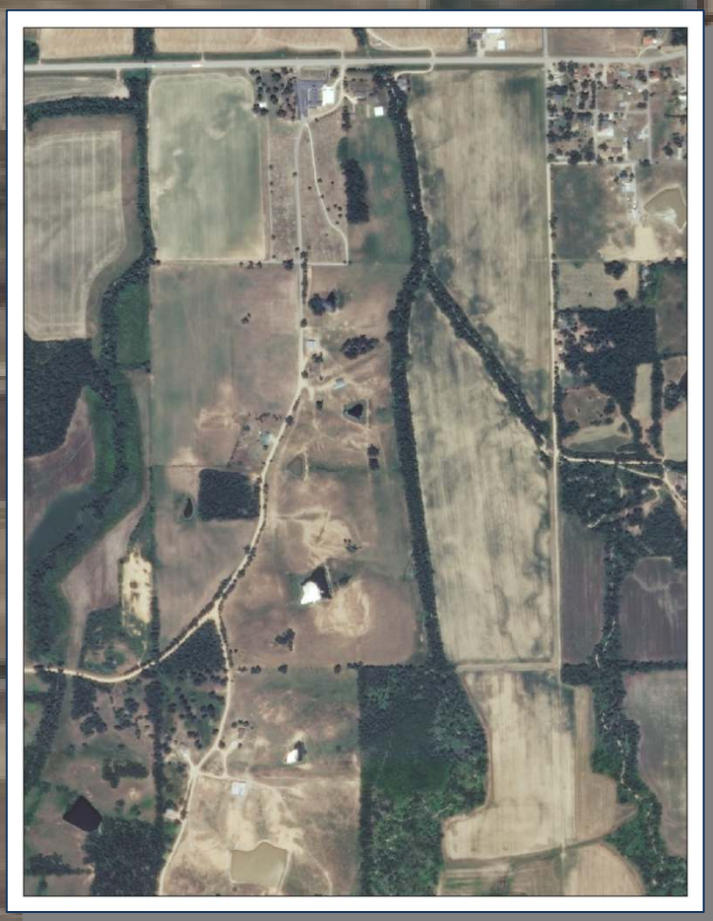

Submitted to:

Department of Geology and Mineral Industries
800 NE Oregon Street, Suite 965
Portland, OR 97232

Submitted by:

Watershed Sciences
421 SW 6th Avenue, Suite 800
Portland, OR 97204

LiDAR Remote Sensing Data Collection:
DOGAMI, New Madrid Study Area

TABLE OF CONTENTS

1. Overview

1.1 Study Area

Watershed Sciences, Inc. has collected Light Detection and Ranging (LiDAR) data of the Oregon New Madrid Study Area for the Oregon Department of Geology and Mineral Industries (DOGAMI). The New Madrid area of interest (AOI) totals 739 square miles (473,049 acres) and the total area flown (TAF) covers 748 square miles (478,410 acres). The TAF acreage is greater than the original AOI acreage due to buffering and flight planning optimization (**Figure 1.1** below). The New Madrid study area covers UTM Zone 15 and UTM Zone 16. All data will be delivered in UTM Zone 15; NAD83 (CORS96); NAVD88 (Geoid 03); Units: meters.

Figure 1.1. *DOGAMI New Madrid Study Area.*

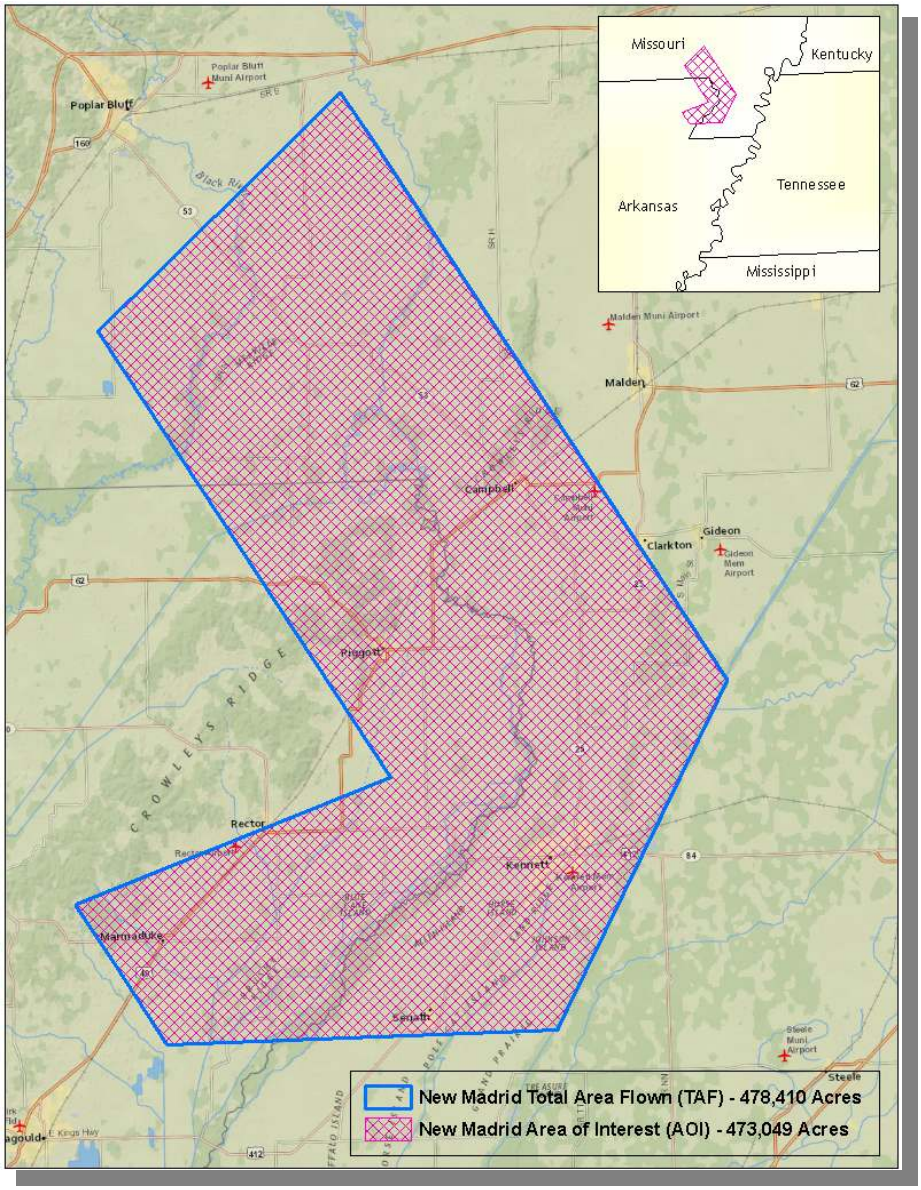

Basemap source: National Geographic

1.2 Geologic Interest in the New Madrid Study Area

The New Madrid seismic zone (NMSZ) has been responsible for producing some of the largest intraplate earthquakes on record (Tuttle et al., 2002). The most recent large magnitude events (~ 7.0 and greater) occurred during the winter of 1811-1812. Studies have also shown that ruptures have occurred in the last 2000 years, at intervals of approximately every 400-600 years, at depths from 4 to 14 km (Kelson et al., 1995; Pollitz et al., 2001). The 1811-1812 NMSZ seismicity produced three major earthquakes (moment magnitudes of M 7-8) followed by several large aftershocks, resulting in the destruction of several settlements along the Mississippi River (Tuttle et al.). The risk of another large magnitude earthquake in this region is of great interest to both local and federal authorities, since several large metropolitan areas are now located in or near the NMSZ. (Recent seismic activity along the New Madrid seismic zone occurred on February 26th 2012 resulting in a 4.0 magnitude quake. Local residents reported shaking that lasted seven seconds long.) Reviews and updates of current earthquake hazard maps and the creation of new maps for the NMSZ have been produced by organizations such as the USGS and academic research institutions.

The mechanism for the occurrence of earthquakes in this region is still widely debated. A study by Braile et al. (1986) revealed that the NMSZ is underlain by a failed rifting event, dating from the late Precambrian. Further results from Braile et al.'s study showed a correlation between the rift and current seismic activity. This correlation indicated that the source of the earthquakes was from slippage along weak zones within the failed rift, caused by the E-W compressive stress of the region, a result of plate motion. Additional studies confirmed the association of the active seismic zone with the failed rift, now named the Reelfoot Rift (Pollitz et al., 2001). During the failed rifting event, emplacement of mafic plutons throughout the crustal column took place. These mafic plutons create a downward pull on the more elastic upper crust. This results in creating a thrust-faulting zone with associated strike-slip faulting (SW-NE trending) cycles, which causes the mafic bodies to sink and in turn, renews the process (Pollitz et al.).

Risk management, hazard mitigation, and the advancement of the body of knowledge in geologic research for the NSMZ support the critical relevance for high accuracy, high resolution environmental data for this area, represented by the present dataset.

1.3 Area Delivered to Date

Table 1.1. Total delivered acreage to date is detailed below.

DOGAMI New Madrid Study Area			
Delivery Date	**Acquisition Dates**	**AOI Acres**	**TAF Acres**
March 30thth, 2012	January 30th – February 26th, 2012	473,049	478,410

Figure 1.2. *New Madrid Delivery area, illustrating the delivered 7.5 minute USGS quads.*

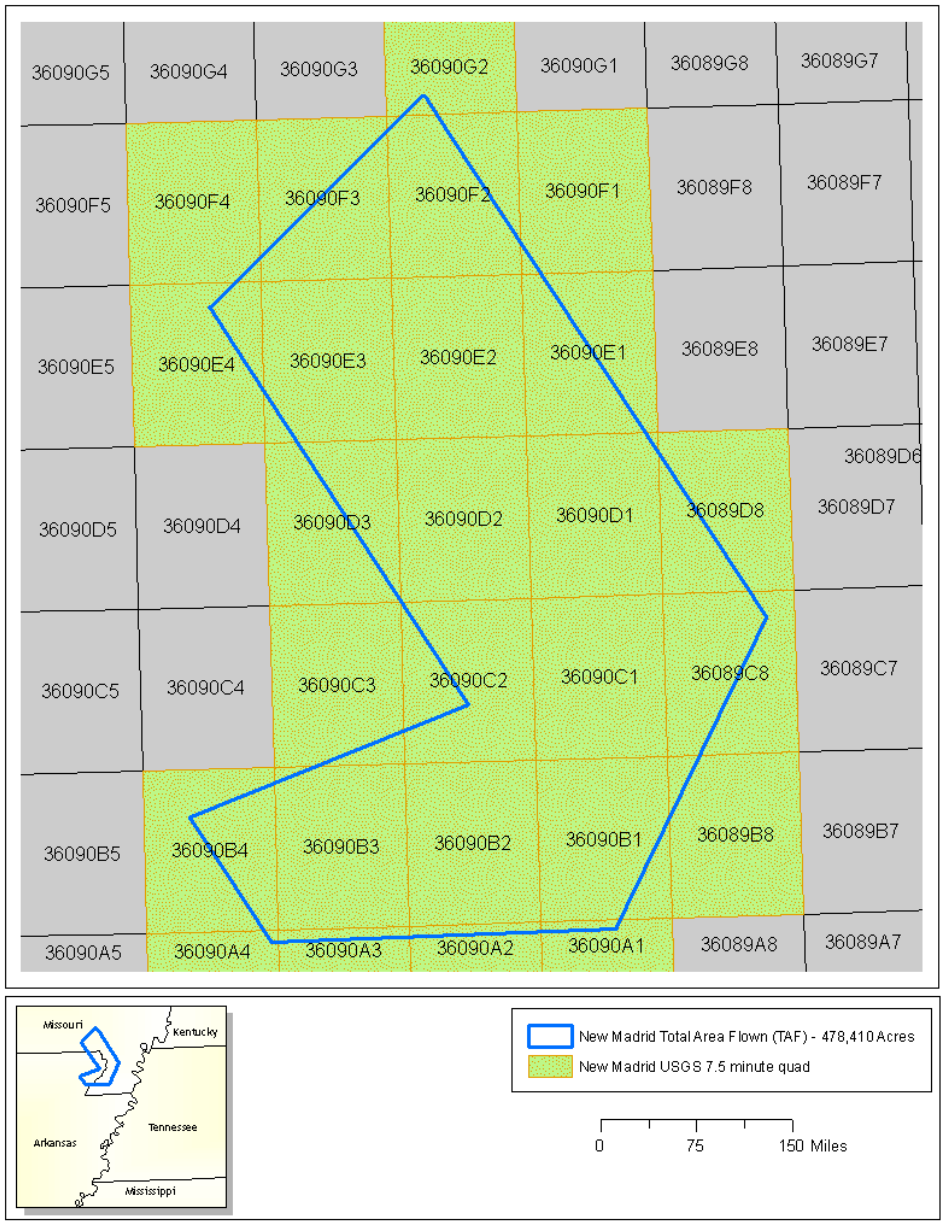

2. Acquisition

2.1 Airborne Survey Overview – Instrumentation and Methods

The LiDAR survey utilized a Leica ALS50 sensor mounted in a Partenavia P.38 aircraft. The systems were set to acquire ≥105,000 laser pulses per second (i.e. 105 kHz pulse rate) and flown at 1300 meters above ground level (AGL), capturing a scan angle of ±12° from nadir[1]. These settings are developed to yield points with an average native density of ≥8 points per square meter over terrestrial surfaces. The native pulse density is the number of pulses emitted by the LiDAR system. Some types of surfaces (i.e. dense vegetation or water) may return fewer pulses than the laser originally emitted. Therefore, the delivered density can be less than the native density and lightly variable according to distributions of terrain, land cover and water bodies.

The presence of widespread inundation for migratory waterfowl corridor habitat as well as standing water from rain events raised concerns for ground model resolution. Native pulse resolution and resulting ground classified point resolution can be reduced by standing surface water, owing to the scattering and absorption properties of water. This ground condition at time of acquisition resulted in the decision to reconfigure the AOI to the southeast, over drier terrain.

Table 2.1 *LiDAR Survey Specifications*

Sensors	Leica ALS50
Survey Altitude (AGL)	1300 m
Pulse Rate	>105 kHz
Pulse Mode	Single
Mirror Scan Rate	52 Hz
Field of View	24° (±12° from nadir)
Roll Compensated	Up to 15°
Overlap	120% (60% Side-lap)

The study area was surveyed with opposing flight line side-lap of ≥60% (≥120% overlap) to reduce laser shadowing and increase surface laser painting. The system allows up to four range measurements per pulse, and all discernable laser returns were processed for the output dataset.

To solve for laser point position, it is vital to have an accurate description of aircraft position and attitude. Aircraft position is described as x, y and z and measured twice per second (2 Hz) by an onboard differential GPS unit. Aircraft attitude is measured 200 times per second (200 Hz) as pitch, roll and yaw (heading) from an onboard inertial measurement unit (IMU).

[1] Nadir refers to the perpendicular vector to the ground directly below the aircraft. Nadir is commonly used to measure the angle from the vector and is referred to a "degrees from nadir".

Figure 2.1. *Actual flightlines for the New Madrid Study Area illustrating the dates flown for processing.*

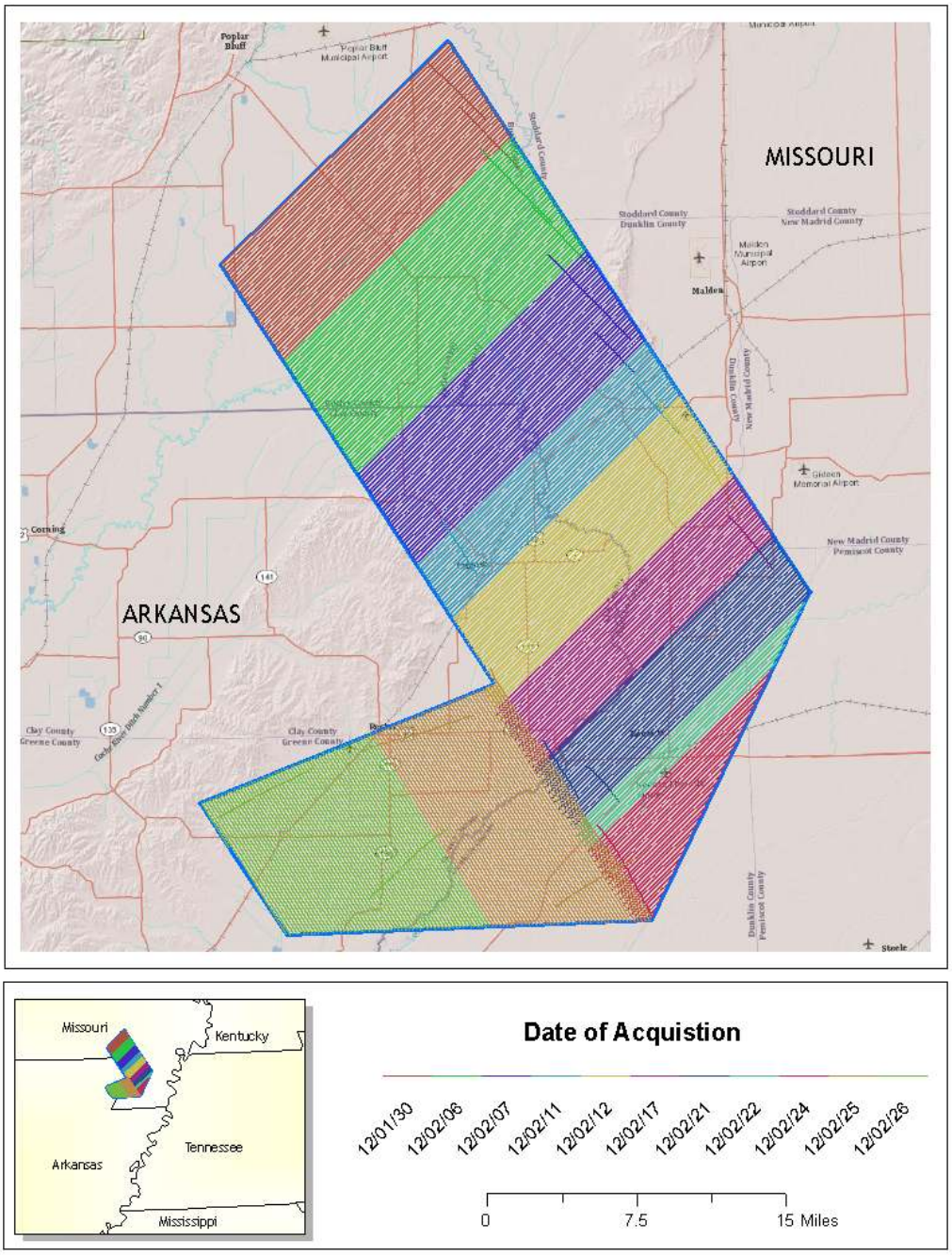

2.2 Ground Survey – Instrumentation and Methods

During the LiDAR survey, static (1 Hz recording frequency) ground surveys were conducted over monuments with known coordinates. Monument coordinates are provided in **Table 2.2** and shown in **Figure 2.2**. After the airborne survey, the static GPS data were processed using triangulation with CORS stations and checked against the Online Positioning User Service (OPUS[2]) to quantify daily variance. Multiple sessions were processed over the same monument to confirm antenna height measurements and reported position accuracy.

2.2.1 Instrumentation

For this study area all Global Navigation Satellite System (GNSS[3]) survey work utilizes a Trimble GPS receiver model R7 with a Zephyr Geodetic antenna with ground plane for static control points. The Trimble GPS R8 unit is used primarily for Real Time Kinematic (RTK) work but can also be used as a static receiver. For RTK data, the collector begins recording after remaining stationary for 5 seconds then calculating the pseudo range position from at least three epochs with the relative error under 1.5 cm horizontal and 2 cm vertical. All GPS measurements are made with dual frequency L1-L2 receivers with carrier-phase correction.

2.2.2 Monumentation

Whenever possible, existing and established survey benchmarks shall serve as control points during LiDAR acquisition including those previously set by Watershed Sciences. In addition to NGS, the county surveyor's offices often establish their own benchmarks. NGS benchmarks are preferred for control points. In the absence of NGS benchmarks, county surveys, Watershed Sciences produces our own monuments. These monuments are spaced at a minimum of one mile and every effort is made to keep these monuments within the public right of way or on public lands. If monuments are required on private property, consent from the owner is required. All monumentation is done with 5/8" x 30" rebar topped with a 2" diameter aluminum cap stamped "Watershed Sciences, Inc.".

[2] Online Positioning User Service (OPUS) is run by the National Geodetic Survey to process corrected monument positions.
[3] GNSS: Global Navigation Satellite System consisting of the U.S. GPS constellation and Soviet GLONASS constellation

2.2.3 Methodology

Each aircraft is assigned a ground crew member with two R7 receivers and an R8 receiver. The ground crew vehicles are equipped with standard field survey supplies and equipment including safety materials. All control points are observed for a minimum of two survey sessions lasting no fewer than 2 hours. At the beginning of every session the tripod and antenna are reset, resulting in two independent instrument heights and data files. Data are collected at a rate of 1Hz using a 10 degree mask on the antenna.

The ground crew uploads the GPS data to the Dropbox website on a daily basis to be returned to the office for Professional Land Surveyor (PLS) oversight, Quality Assurance/Quality Control (QA/QC) review and processing. OPUS processing triangulates the monument position using 3 CORS stations resulting in a fully adjusted position. CORPSCON[4] 6.0.1 software is used to convert the geodetic positions from the OPUS reports. After multiple days of data have been collected at each monument, accuracy and error ellipses are calculated. This information leads to a rating of the monument based on FGDC-STD-007.2-1998[5] Part 2 **(Table 2.2)** at the 95% confidence level.

All RTK measurements are made during periods with a Position Dilution of Precision (PDOP) of ≤ 3.0 and in view of at least six satellites by the stationary reference and roving receiver. RTK positions are collected on 20% of the flight lines and on bare earth locations such as paved, gravel or stable dirt roads, and other locations where the ground is clearly visible (and is likely to remain visible) from the sky during the data acquisition and RTK measurement period(s). In order to facilitate comparisons with LiDAR measurements, RTK measurements are not taken on highly reflective surfaces such as center line stripes or lane markings on roads. RTK points are taken no closer than one meter to any nearby terrain breaks such as road edges or drop offs. In addition, it is desirable to include locations that can be readily identified and occupied during subsequent field visits in support of other quality control procedures described later. Examples of identifiable locations would include manhole and other flat utility structures that have clearly indicated center points or other measurement locations. In the absence of utility structures, a PK nail can be driven into asphalt or concrete and marked with paint.

Multiple differential GPS units are used in the ground based real-time kinematic (RTK) portion of the survey. To collect accurate ground surveyed points, a GPS base unit is set up over monuments to broadcast a kinematic correction to a roving GPS unit. The ground crew uses a roving unit to receive radio-relayed kinematic corrected positions from the base unit. This RTK survey allows precise location measurement ($\sigma \leq 1.5$ cm). **Figure 2.3** shows subsets of these RTK locations.

[4] U.S. Army Corps of Engineers , Engineer Research and Development Center Topographic Engineering Center software

[5] Federal Geographic Data Committee Draft Geospatial Positioning Accuracy Standards

Table 2.2. *Base Station Surveyed Coordinates, (NAD83/NAVD88, OPUS corrected) used for kinematic post-processing of the aircraft GPS data for the New Madrid Study Area.*

	Datum NAD83		GRS80
Base Stations ID	**Latitude (North)**	**Longitude (West)**	**Ellipsoid Height (m)**
N_MAD_01	36 37 07.89791	90 16 31.18331	65.976
N_MAD_02	36 34 12.74584	90 10 05.09200	66.067
N_MAD_03	36 31 37.75539	90 06 48.85428	68.083
N_MAD_04	36 25 08.59992	90 10 11.89579	58.588
N_MAD_05	36 18 33.75410	90 00 27.88090	53.674
N_MAD_06	36 23 18.76269	90 03 51.22480	59.864
N_MAD_09	36 11 07.37502	90 03 01.23795	48.730
N_MAD_10	36 10 37.00199	90 17 06.74713	48.662
N_MAD_11	36 13 26.41215	90 11 44.14806	49.979
N_MAD_12	36 10 15.14757	90 24 37.05505	55.758

Figure 2.2. *Base stations for the New Madrid Study Area.*

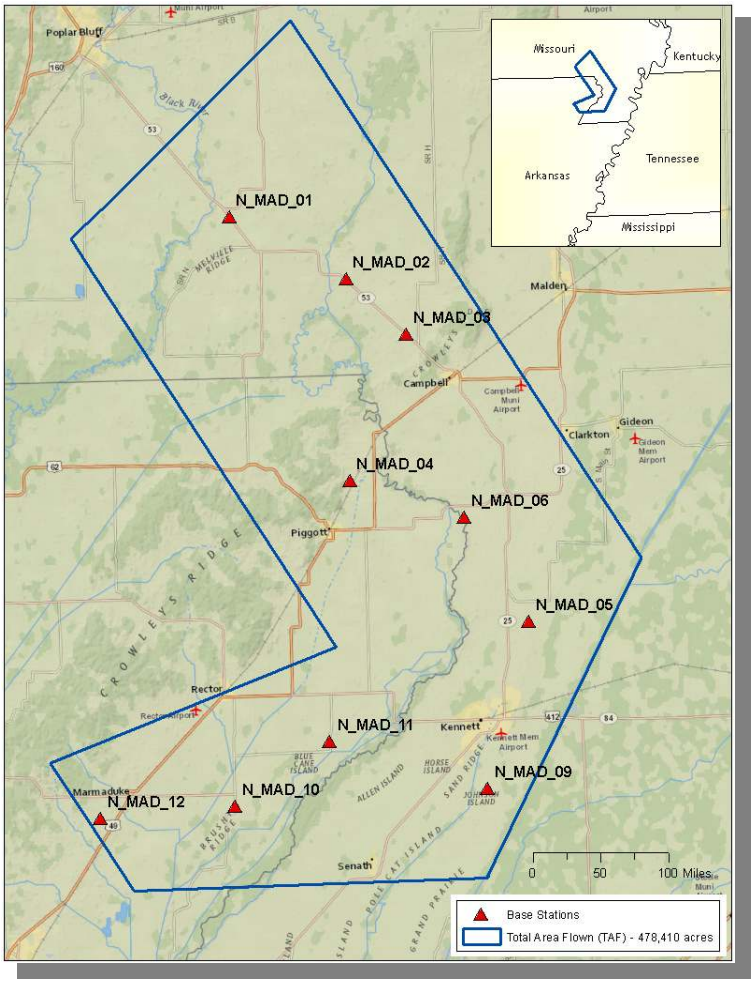

Basemap source: National Geographic

2.2.4 Monument Accuracy

FGDC-STD-007.2-1998[6] at the 95% confidence level for this project:
St Dev $_{NE}$: 0.010 m
St Dev $_{z}$: 0.020 m

2.2.5 RTK Point Data

For data delivered to date 7,463 RTK (Real-time kinematic) points were collected in the study area.

Figure 2.3 shows detailed views of selected RTK locations for the area delivered to date.

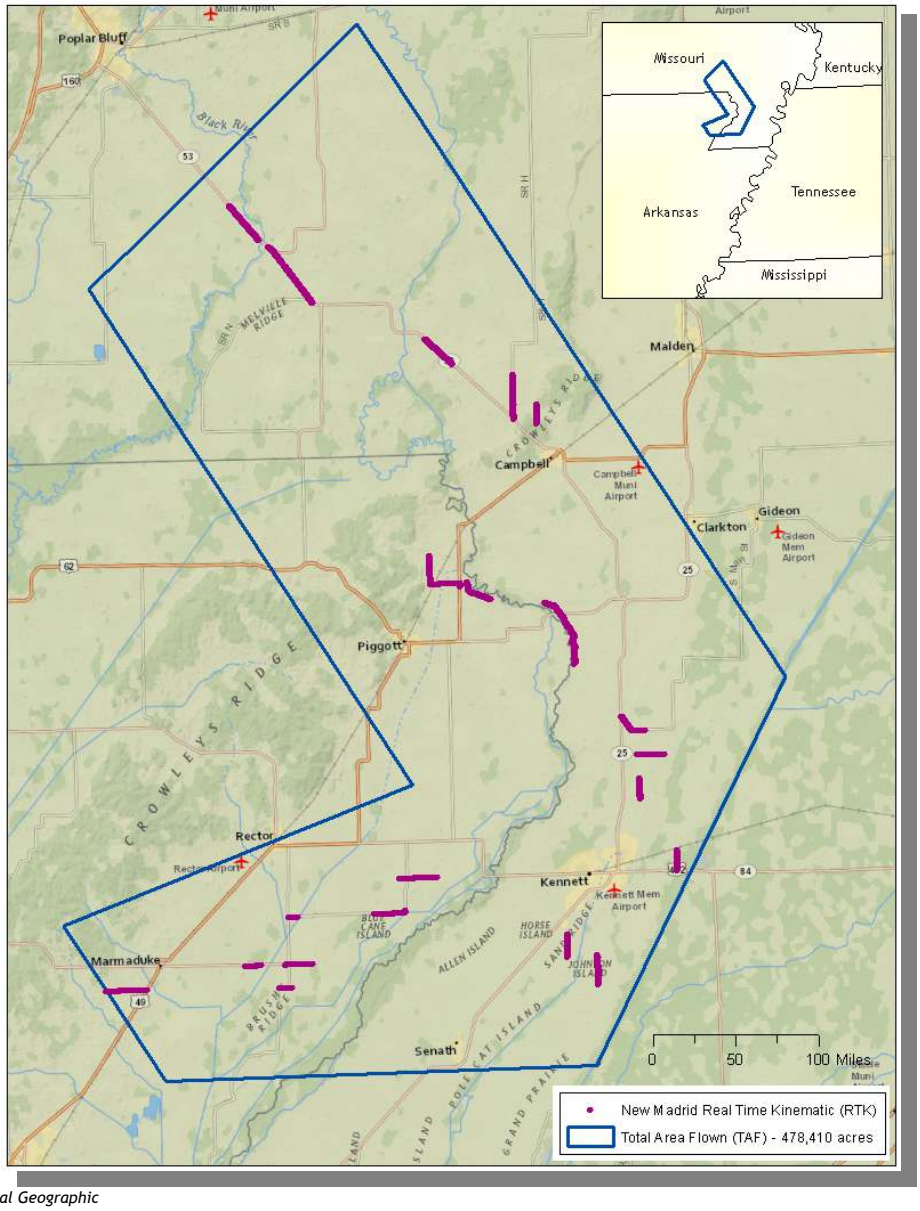

Basemap source: National Geographic

[6] Federal Geographic Data Committee Draft Geospatial Positioning Accuracy Standards (Part 2 table 2.1)

Figure 2.4. *Selected RTK point locations in the study area; images are NAIP orthophotos.*

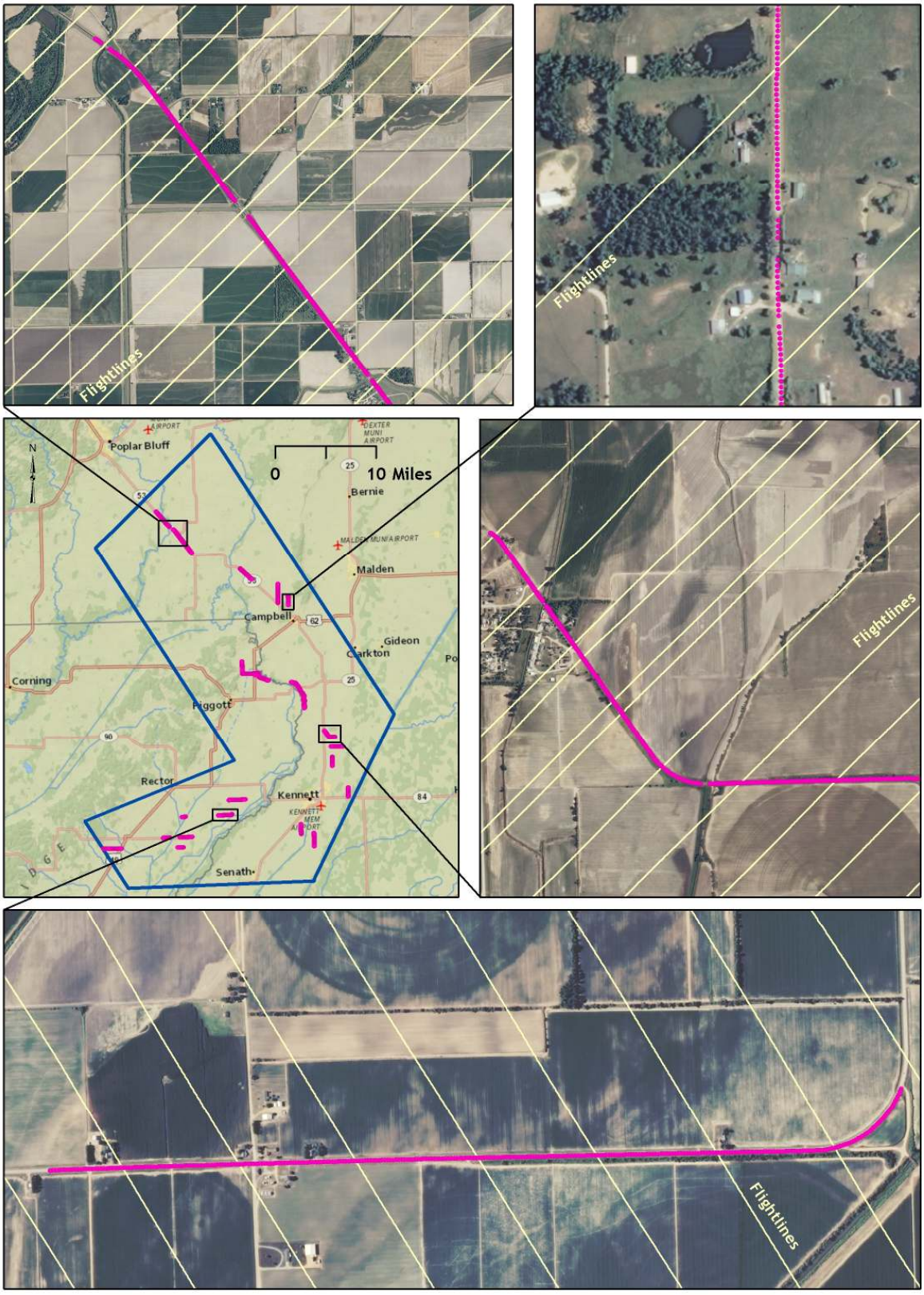

3. Accuracy

3.1 Relative Accuracy

Relative Accuracy Calibration Results

Relative accuracy refers to the internal consistency of the data set and is measured as the divergence between points from different flightlines within an overlapping area. Divergence is most apparent when flightlines are opposing. When the LiDAR system is well calibrated the line to line divergence is low (<10 cm). Internal consistency is affected by system attitude offsets (pitch, roll and heading), mirror flex (scale), and GPS/IMU drift.

Relative accuracy statistics shown in **Figures 3.2 and 3.3** are based on the comparison of 372 flightlines and over 5 billion points. Relative accuracy is reported for the portion of the study area shown in **Figure 3.1** below.

- Project Average = 0.01 m
- Median Relative Accuracy = 0.01 m
- 1σ Relative Accuracy = 0.01m
- 2σ Relative Accuracy = 0.01 m

Figure 3.1. *Relative Accuracy Covered Area.*

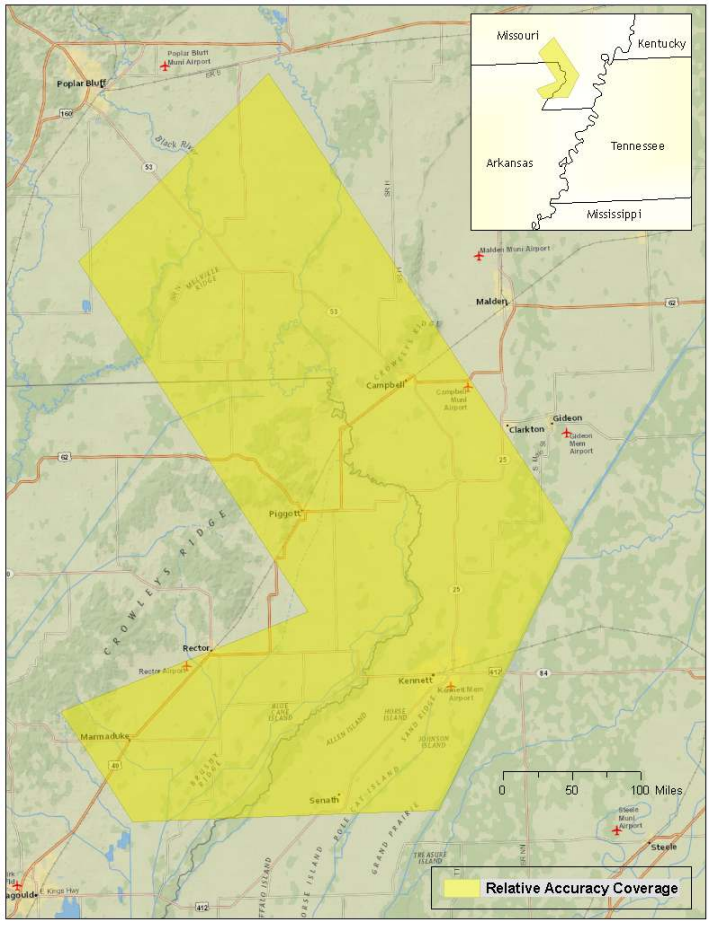

Basemap source: National Geographic

Figure 3.2. *Statistical relative accuracies, non slope-adjusted.*

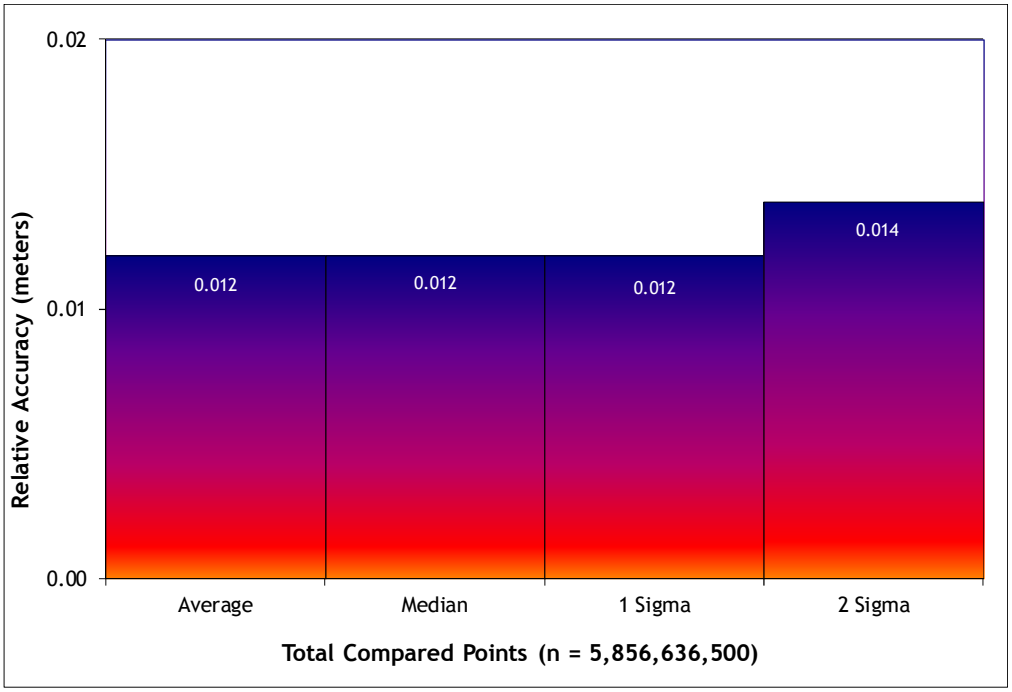

Figure 3.3. *Percentage distribution of relative accuracies, non slope-adjusted.*

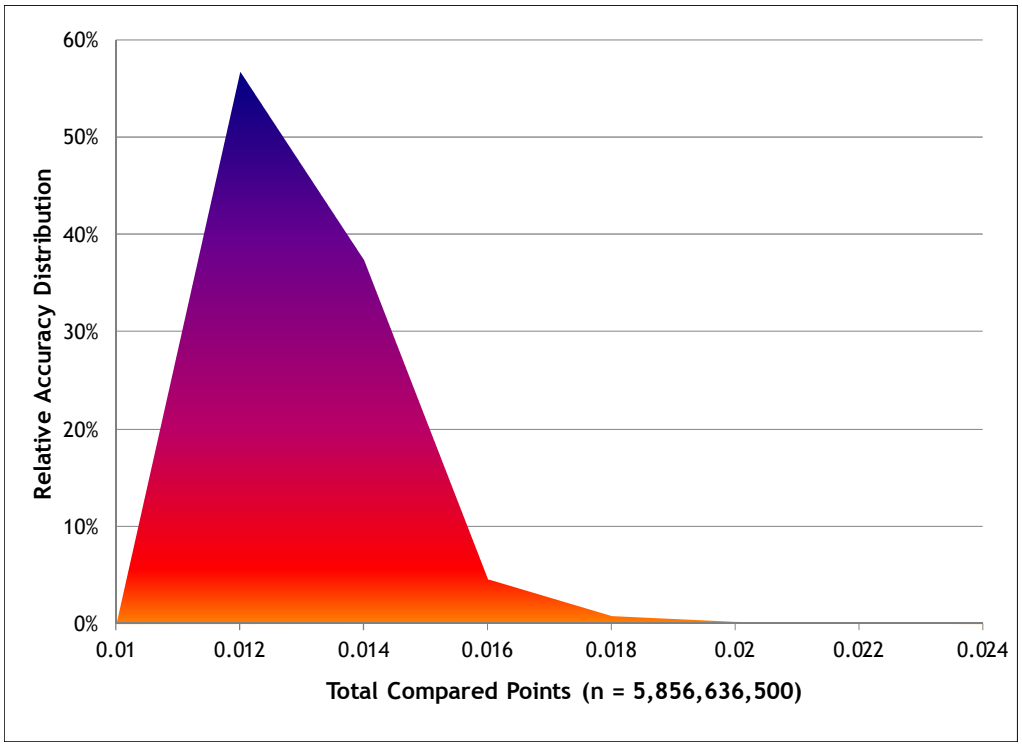

3.2 Fundamental Vertical Accuracy

FVA accuracy reporting is designed to meet guidelines presented in the National Standard for Spatial Data Accuracy (NSSDA) (FGDC, 1998). FVA compares known RTK ground survey points to the closest laser point. FVA uses ground control points in open areas where the LiDAR system has a "very high probability" that the sensor will measure the ground surface and is evaluated at the 95% percentile of $RMSE_{Z.}$ For the New Madrid Study Area, 7,463 RTK points were collected for data delivered to date.

For this project, no independent survey data were collected, nor were reserved points collected for testing. As such, vertical accuracy statistics are reported as "Compiled to Meet," in accordance with the ASPRS Guidelines for Vertical Accuracy Reporting for LiDAR Data V1.0 (ASPRS, 2004). Fundamental Vertical accuracy is reported for the portion of the study area shown in **Figure 3.4** and reported in **Table 3.1** below. Histogram and absolute deviation statistics are reported in **Figures 3.5 and 3.6**.

Table 3.1. *Fundamental Vertical Accuracy – Deviation between laser points and RTK survey points.*

Sample Size (n): 7,463	
Root Mean Square Error (RMSE): 0.03 m	
Fundamental Vertical Accuracy: Compiled to Meet 0.33 ft. (0.10m) fundamental vertical accuracy at 95% confidence level (1.96 x $RMSE_z$) in	
Standard Deviations	**Deviations**
1 sigma (σ): 0.02 m	**Minimum Δz:** -0.08
2 sigma (σ): 0.03 m	**Maximum Δz:** 0.07 m
	Average Δz: -0.01

Figure 3.4. *Area represented by Fundamental Vertical Accuracy statistics.*

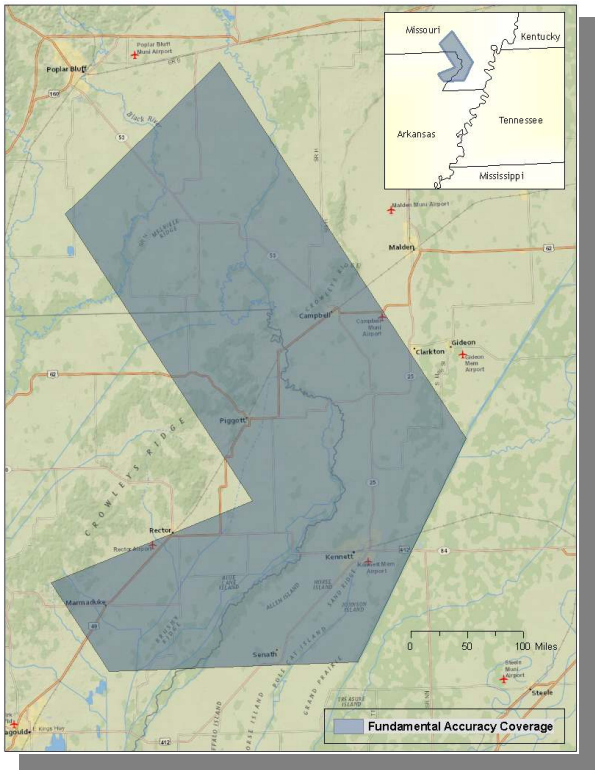

Figure 3.5. *New Madrid Study Area fundamental vertical accuracy histogram statistics*

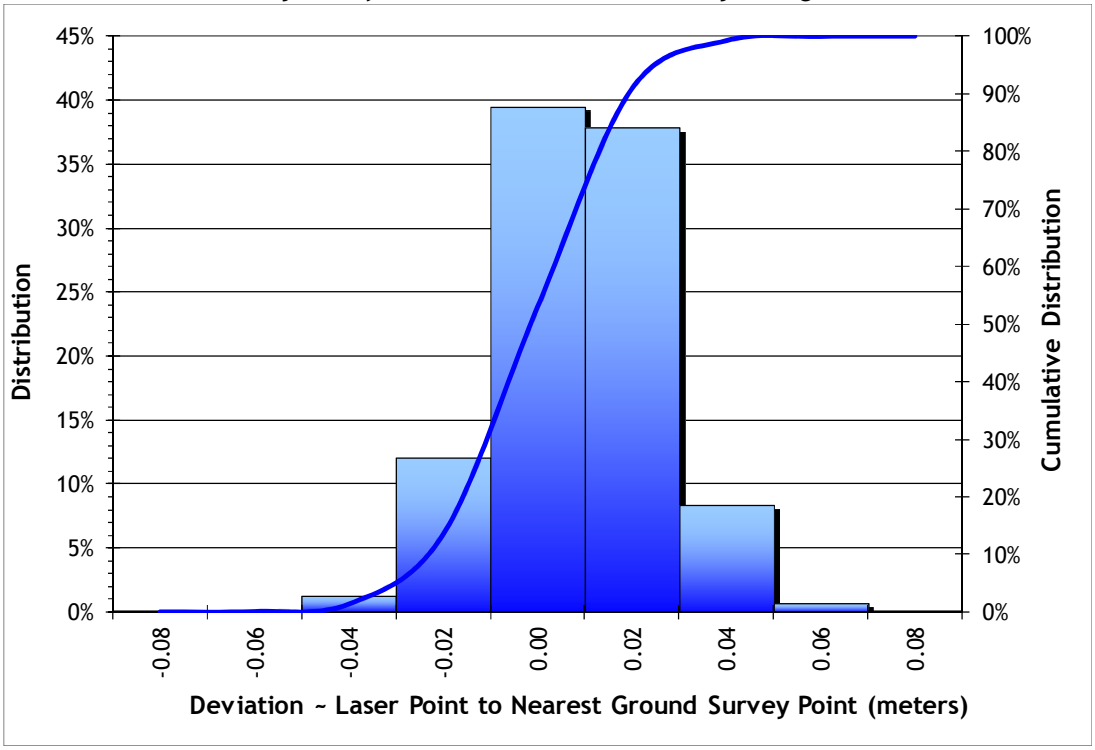

Figure 3.6. *New Madrid Study Area point absolute vertical deviation statistics.*

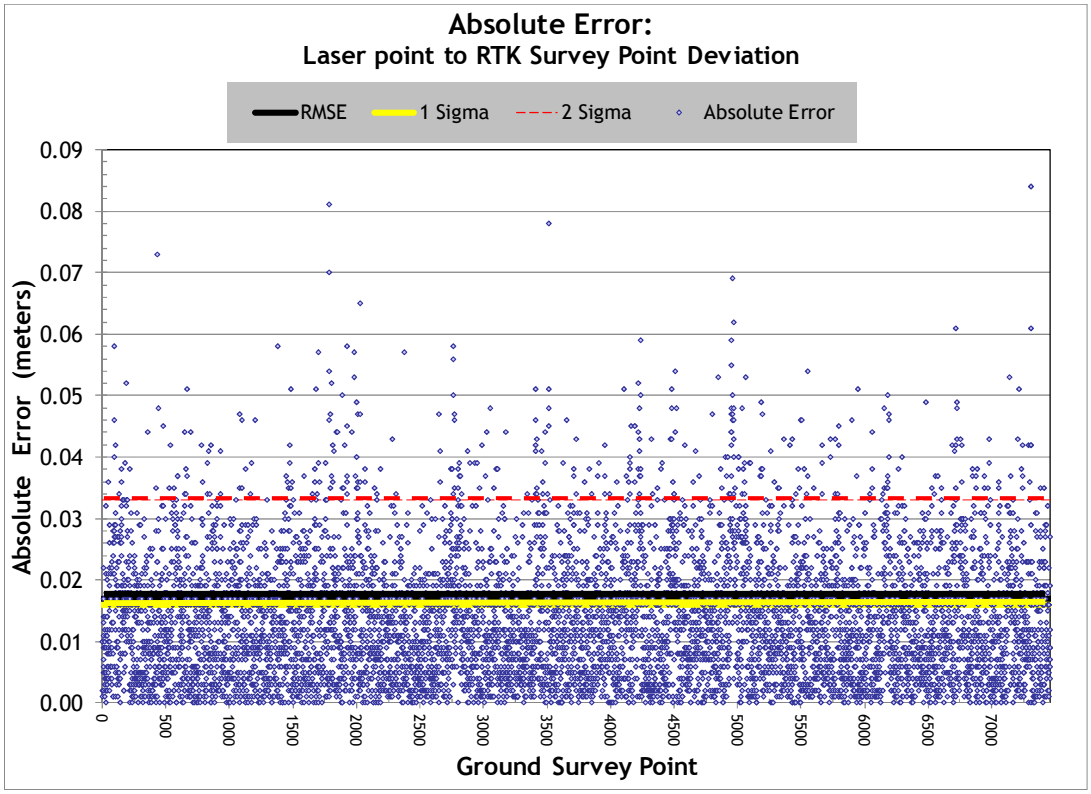

4. Data Density/Resolution

Some types of surfaces (i.e. dense vegetation or water) may return fewer pulses than the laser originally emitted. Therefore, the delivered density can be less than the native density and vary according to terrain, land cover and water bodies. Density histograms and maps (**Figures 4.1 – 4.4**) have been calculated based on first return laser point density and ground-classified laser point density.

Table 4.1. *Average density statistics for New Madrid Study Area data delivered to date.*

Average Pulse Density (per square m)	Average Ground Density (per square m)
8.64	3.06

Figure 4.1. *Histogram of first return laser point density for data delivered to date.*

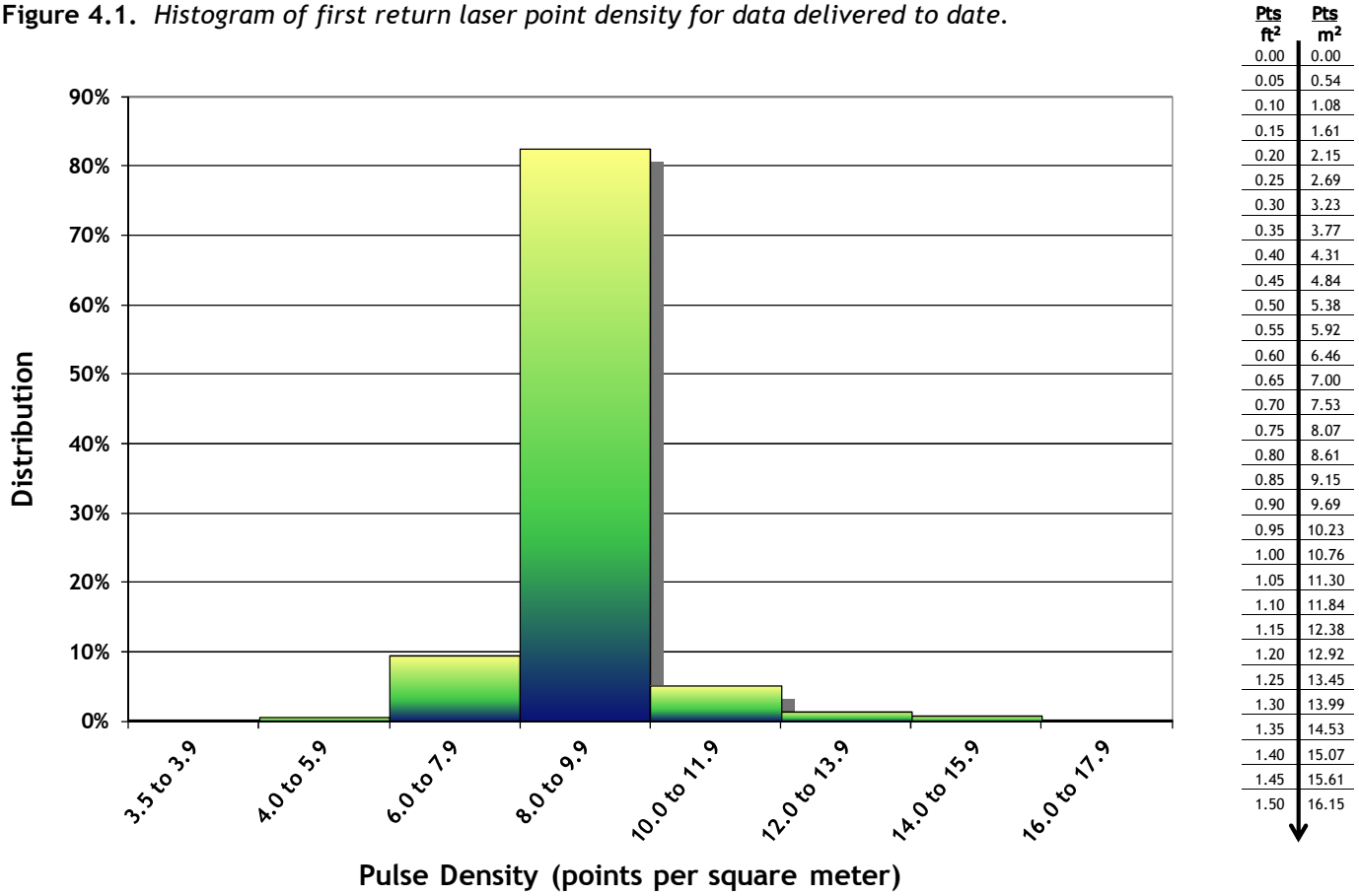

Figure 4.2. *First return laser point densities per 0.75' USGS Quad for data delivered to date.*

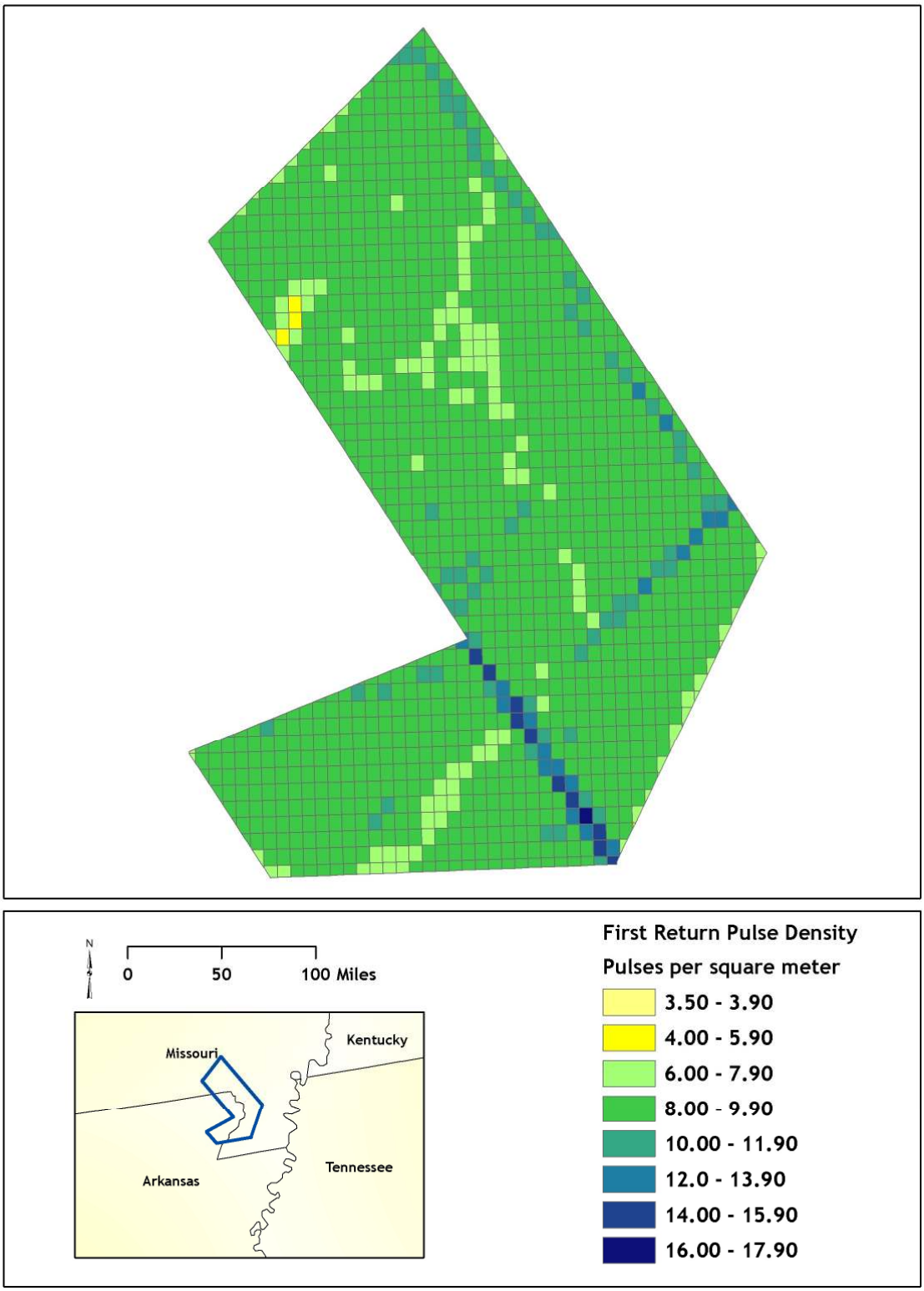

Figure 4.3. Decreased first return point densities are due to the low percentage of points returned over water. High density strips in data are due to the overlapping of flighlines (shown in bottom right).

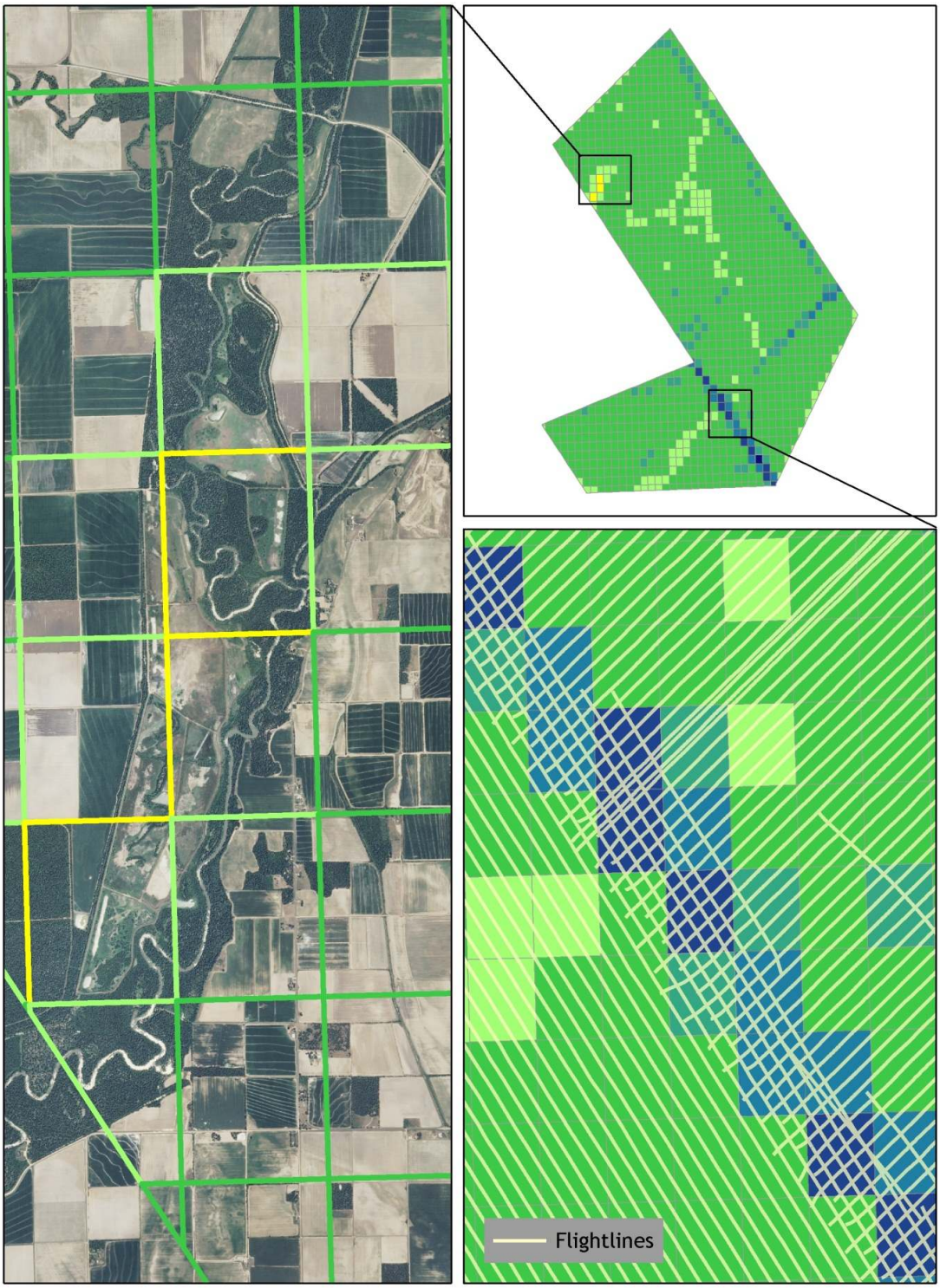

Ground classifications were derived from ground surface modeling. Classifications were performed by reseeding of the ground model where it was determined that the ground model failed, usually under dense vegetation and/or at breaks in terrain, steep slopes and at bin boundaries.

Figure 4.4. *Histogram of ground-classified laser point density for data delivered to date.*

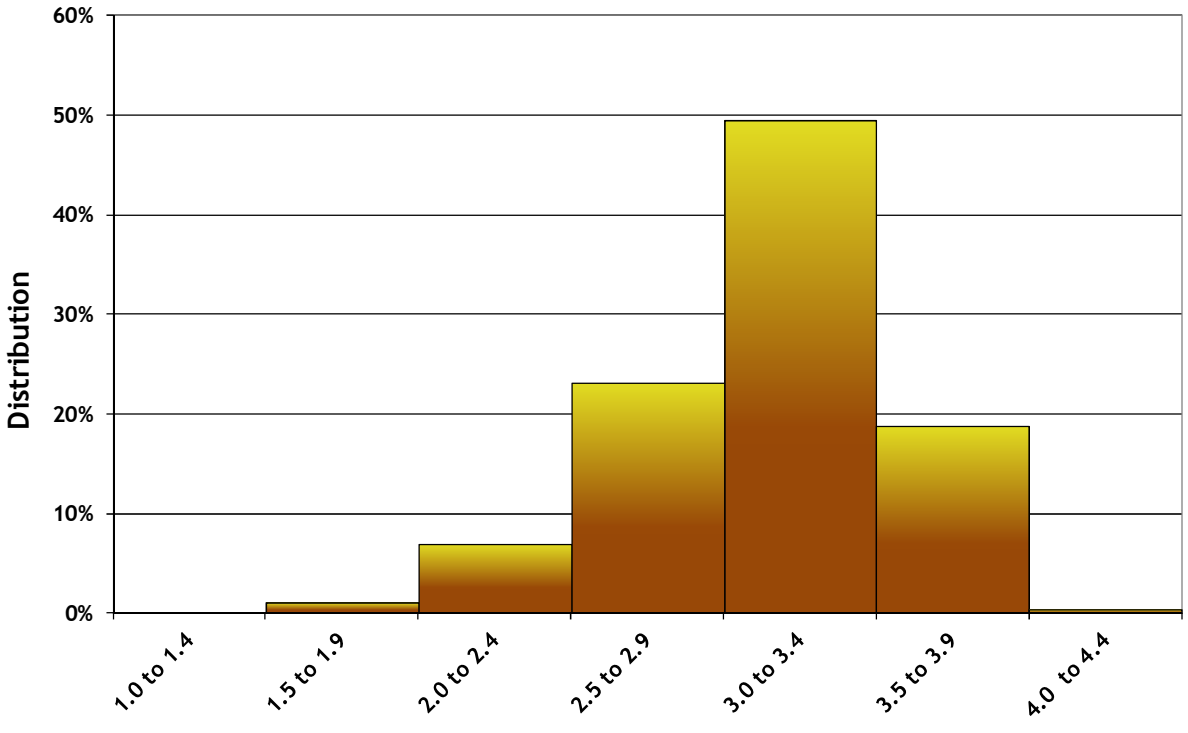

Pts ft²	Pts m²
0.00	0.00
0.05	0.54
0.10	1.08
0.15	1.61
0.20	2.15
0.25	2.69
0.30	3.23
0.35	3.77
0.40	4.31
0.45	4.84
0.50	5.38
0.55	5.92
0.60	6.46
0.65	7.00
0.70	7.53
0.75	8.07
0.80	8.61
0.85	9.15
0.90	9.69
0.95	10.23
1.00	10.76
1.05	11.30
1.10	11.84
1.15	12.38
1.20	12.92
1.25	13.45
1.30	13.99
1.35	14.53
1.40	15.07
1.45	15.61
1.50	16.15

Figure 4.5. *Ground-classified laser point density per 0.75' USGS Quad for data delivered to date.*

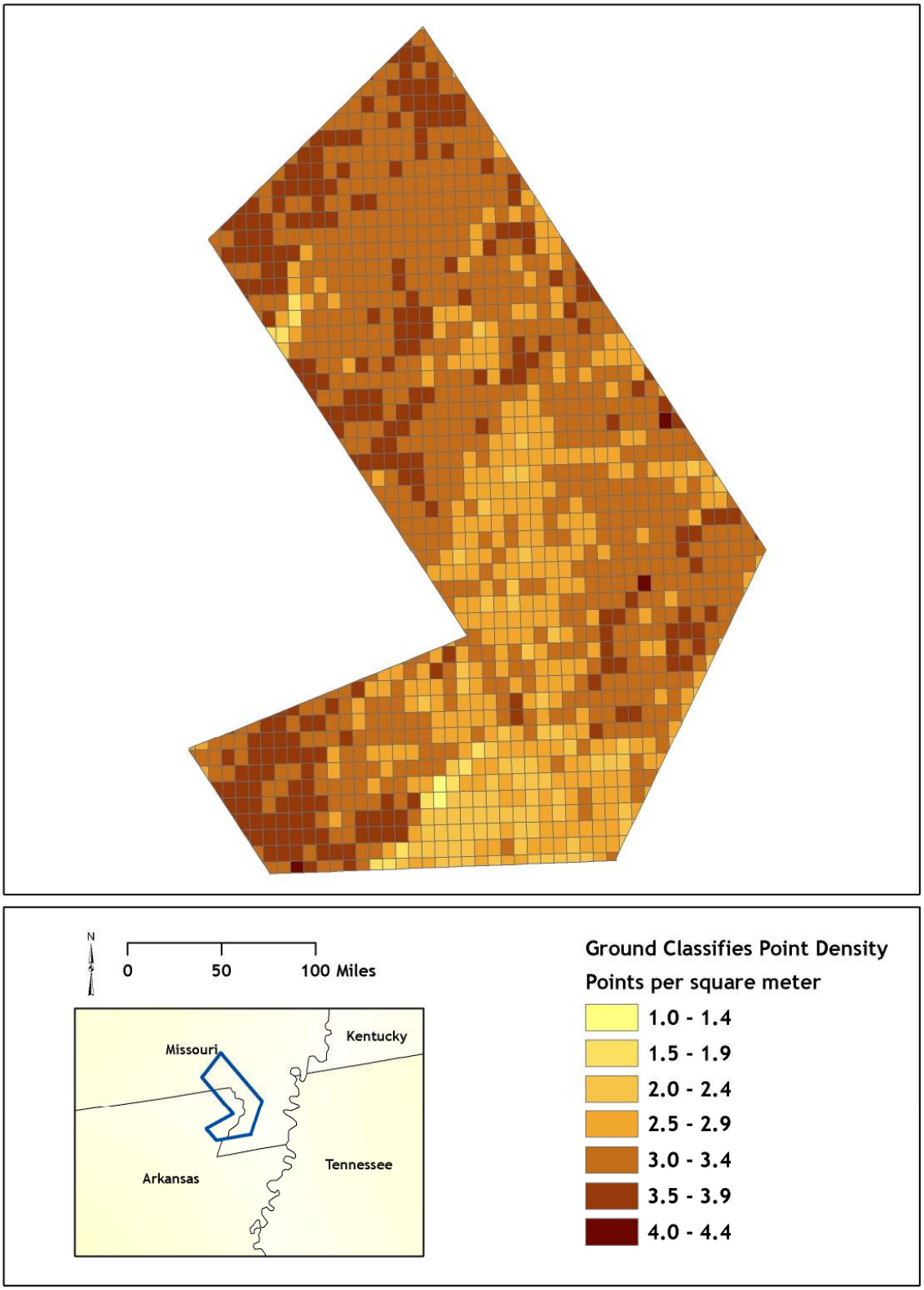

Pts ft²	Pts m²
0.00	0.00
0.05	0.54
0.10	1.08
0.15	1.61
0.20	2.15
0.25	2.69
0.30	3.23
0.35	3.77
0.40	4.31
0.45	4.84
0.50	5.38
0.55	5.92
0.60	6.46
0.65	7.00
0.70	7.53
0.75	8.07
0.80	8.61
0.85	9.15
0.90	9.69
0.95	10.23
1.00	10.76
1.05	11.30
1.10	11.84
1.15	12.38
1.20	12.92
1.25	13.45
1.30	13.99
1.35	14.53
1.40	15.07
1.45	15.61
1.50	16.15

5. Citations

Braile, L.W., Hinze, W.J., Keller, G.R., Lidiak, E.G., and Sexton, J.L. (1986). Tectonic Development of the New Madrid Rift Complex, Mississippi Embayment, North America. *Tectonophysics*, 131, 1-21.

Federal Geographic Data Committee, 1998. Geospatial Positioning Accuracy Standards Part 3: National Standard for Spatial Data Accuracy. Subcommittee for Base Cartographic Data, 25p.

Flood, M, (Ed.), 2004. ASPRS Guidelines-Vertical Accuracy Reporting for Lidar Data, V1.0. American Society for Photogrammetry and Remote Sensing (ASPRS) Lidar Committee, 20p.

Kelson, K.I., Simpson, G.D., Arsdale, R.B., Haraden, C.C., and Lettis, W.R. (1996). Multiple late Holocene earthquakes along the Reelfoot fault, central New Madrid seismic zone. *Journal of Geophysical Research,* 101, 6151-6170.

Pollitz, F.F., Kellogg, L., and Burgmann, R. (2001). A mechanism for stress concentration at the New Madrid seismic zone. *Bulletin of the Seismological Society of America*, April-2001.

Tuttle, M.P., Schweig, E.S., Sims, J.D., Lafferty, R.H., Wolf, L.W., and Haynes, M.L. (2002). The Earthquake Potential of the New Madrid Seismic Zone. *Bulletin of the Seismological Society of America,* 92, 2080-2089.

U.S. Geological Survey Land Cover Institute. "NLCD Land Cover Class Definitions." 17 March, 2011. http://landcover.usgs.gov/classes.php.

6. Selected Imagery

Figure 6.1. Synform and antiform geologic structures surrounding Pollard, Clay County, Arkansas. View to the East. Image is a LiDAR point cloud colored with RGB values from NAIP imagery.

Figure 6.2. Synform and antiform geologic structures surrounding Highway 62 and Pollard, Clay County, Arkansas. View to the Southeast. Image is a LiDAR point cloud colored with RGB values from NAIP imagery.

Figure 6.3. Possible antiforms located southeast of Holcomb, Dunklin County, Missouri. View to the North. Image is a LiDAR point cloud colored with RGB values from NAIP imagery.

Figure 6.4 Possible Antiforms surrounding Intersection of County Road 419 and Highway 25. Dunklin County, Missouri. View to the South. Image is a LiDAR point cloud colored with RGB values from NAIP imagery.